Glass transition in metallic glasses: A microscopic model of topological fluctuations in the bonding network

T. Egami,[1,2,3] S. J. Poon,[4] Z. Zhang,[2] and V. Keppens[1,2]
[1]*Oak Ridge National Laboratory, Oak Ridge, Tennessee 37831, USA*
[2]*Department of Materials Science and Engineering, University of Tennessee, Knoxville, Tennessee 37996, USA*
[3]*Department of Physics and Astronomy, University of Tennessee, Knoxville, Tennessee 37996, USA*
[4]*Department of Physics, University of Virginia, Charlottesville, Virginia 22904, USA*
(Received 5 February 2007; published 9 July 2007)

Understanding of the structure and dynamics of liquids and glasses at an atomistic level lags well behind that of crystalline materials, even though they are important in many fields. Metallic liquids and glasses provide an opportunity to make significant advances because of its relative simplicity. We propose a microscopic model based on the concept of topological fluctuations in the bonding network. The predicted glass transition temperature, T_g, shows excellent agreement with experimental observations in metallic glasses. To our knowledge this is the first model to predict the glass transition temperature quantitatively from measurable macroscopic variables.

DOI: 10.1103/PhysRevB.76.024203 PACS number(s): 64.70.Pf, 61.20.Gy, 66.20.+d

I. INTRODUCTION

The atomic structure and dynamics of liquids and glasses are much less understood today compared to those of crystalline solids, for which the first-principle theories can answer many questions, and even make some predictions. In particular the nature of the glass and glass transition is considered to be one of the most challenging problems.[1,2] In dealing with liquids and glasses we do not enjoy the benefit of the translational symmetry and resultant Bloch theorem, and have to face directly the complex many-body interactions. This frustrates most of conventional approaches which rely on the Bloch theorem. For this reason much of the recent progresses have been made in the theories of mesoscopic scale, in particular the mode-coupling theory (MCT).[3,4] In the MCT the dynamics of liquid is described by nonlinear hydrodynamic equations with variables chosen to fit certain experimental results. While the physics of nonlinear coupling and feedback effect is very well described by the MCT, the atomistic underpinning of such interactions is usually disregarded as less important details. This may well be unavoidable for very complex fluids such as macromolecular systems, but for simpler liquids it should be possible to improve and deepen our understanding of the atomic level mechanisms. For this purpose we propose a unique approach based on the description of topological fluctuations in the atomic bonding network to describe the thermal evolution of the structure of metallic liquids and glasses. We show that the theory leads to expressions of the glass transition temperature that agree well with experimental observations in metallic glasses. A key idea to this success is to focus not on the dynamics of each atom but on the collective dynamics of the nearest neighbor shells, and take into account the dependence on Poisson's ratio that characterizes the interaction between local density and shear fluctuations.

In order to describe and understand the atomic structure of liquids and glasses the choice of the key concepts or parameters that connect the bare atomic coordinates with the properties is critical. The most widely used one is the atomic pair-distribution function (PDF), which can be directly determined through diffraction experiments.[5] However, the physical properties usually depend on more collective environment of atoms. For this purpose the Voronoi polyhedral analysis is frequently used.[6,7] The underlying assumption of this approach is that the relative positions of the nearest neighbor atoms are most important in determining the behavior of an atom, and thus we should focus on the topology of atomic connectivity. This approach is natural for covalent glasses, but it is also applicable to metallic and ionic liquids and glasses as well, since the first nearest neighbors are fairly well defined by the first peak in the pair-density function.[8] However, the local properties depends not only on the local topology but also on the geometrical distortion of the local polyhedra of nearest neighbor atoms. In order to include this effect we introduced the method of describing the local atomic packing in terms of atomic-level stresses.[9]

In the liquid state the topology of atomic connectivity is not static, but is fluctuating. Earlier we introduced basic concepts of describing thermal effects by using the fluctuations in atomic-level stresses and strains as local variables.[10,11] In this way it became possible to connect the local topology to the local energy landscape. In the present work we make connections between the local fluctuations and the criterion of the local topological instability[12,13] to discuss the glass transition. The results are compared to the experimental data, demonstrating that the theory is capable of quantitatively describing the glass transition temperature from measurable quantities (atomic volume and elastic moduli) with minimum assumptions.

II. LOCAL TOPOLOGY OF ATOMIC LIQUIDS AND THEIR FLUCTUATIONS

An obvious choice of a parameter to characterize the local topology of atomic connectivity is the local coordination number, N_C, or the number of first neighbors. In a glass structure represented, for instance, by the dense random packed (DRP) structure[14] N_C varies locally. We note that the local variation in N_C has a very direct physical meaning: Consider a void surrounded by a certain number of atoms, N_C. It is obvious that when the void is large N_C is also large. One would simply argue that N_C should be proportional to the square of the radius of the void, r_v, since near neighbors would fill the inner surface of the void with a certain constant packing fraction. Indeed for a system with a short-range pairwise potential it was possible to derive a quantitative expression for the ideal coordination number of an impurity A atom with the radius r_A embedded in the metallic glass of B atoms with the radius r_B (Ref. 15)

$$N_C(x) = 4\pi\left(1 - \frac{\sqrt{3}}{2}\right)(1+x)[1+x+\sqrt{x(x+2)}], \qquad (1)$$

where $x=r_A/r_B$. This equation was derived by a heuristic argument and is not meant to be a rigorous mathematic statement. However, its approximate accuracy, as proven by a computer simulation,[15] is sufficient for the purpose of the argument developed here.

The inverse of Eq. (1), $x(n)=N_C^{-1}(n)$, specifies the ideal size of an atom, $x(n)r_B$, to fit an atomic site, or a void, with N_C. If the radius of an atom is larger than $x(n)r_B$, the atom will be under compression, while if it is too small it will be under dilatational (negative) pressure. Thus the misfit between the local topology and the atomic size can be translated into a local stress, and then to a local elastic energy. For instance if an icosahedron cluster is formed with 13 atoms with an equal size, the central atom will be under compression, while the peripheral atoms will be under shear stresses, as expected from the fact that in the icosahedron the distance from the center to the apex is shorter than the distance between apexes. Indeed Eq. (1) gives $N_C^{-1}(12)=0.958$.[16] The fact $N_C(1)>12$ reflects the frustration of the icosahedral environment as discussed, for instance, by Nelson.[17]

Now the converse of this situation is even more interesting. Note that $N_C(x)$ defined by Eq. (1) is a continuous function of x, while the actual local coordination has to be integral. This means only at special values of x ($=x_n$) at which $N_C(x_n)=n$, an integer, the Eq. (1) can be satisfied, while in-between it can be achieved only in the average. For instance if $N_C=n+m/k$ ($m<k$), it is possible to achieve the ideal coordination in the average, by forming a crystal with k-m number of atomic sites with $N_C=n$ and m sites with $N_C=n+1$. But every site is under some pressure, negative for $N_C=n$ and positive for $N_C=n+1$, costing elastic energies associated with local distortion. For a monoatomic system ($x=1$), $N_C(1)=4\pi=12.56\ldots$, an irrational number. Thus this condition can be satisfied only with a crystal with an infinitely large unit cell, possibly with a quasicrystal, and the DRP structure becomes a strong competitor as an alternative.

Thus in the DRP structure in which Eq. (1) describes the ideal coordination number, the local energy landscape of an atom, $E(x)$, is an oscillating function of x, with minima at each value of x_n, since only then the actual coordination number, which is an integer, is ideal. Then if in the Gedanken experiment the size of an atom A is inflated and the value of x is continuously increased, N_C will increase stepwise since N_C is always an integer, and the local topology is changed every time the coordination number is increased. This point of topological change defines the critical strain for the local topological instability, which is related to the Lindemann's criterion for melting.[13] It is the strain that corresponds to the change in the equilibrium N_C by about 0.5. This concept of topological instability was successfully applied to predict the compositional limit for glass formation in binary glasses.[12]

In order to describe the misfit between the ideal local packing and the actual local atomic structure we introduced the local atomic level pressure of an ith atom, $p(i)$, as the local increase in the energy due to volume strain as

$$p(i) = \frac{1}{V_i}\sum_j \boldsymbol{f_{ij}} \cdot \boldsymbol{r_{ij}}, \qquad (2)$$

where V_i is the local atomic volume of the ith atom, $\boldsymbol{f}_{ij}$ is the two-body force, and $\boldsymbol{r}_{ij}$ is the separation, between the atom i and j.[9] The local pressure thus defined is indeed correlated with the local coordination number, N_C.[10] The local topology of the atomic bonds can be described not only by the number of bonds around an atom, N_C, but also by the anisotropy of the bond connectivity. For instance a hoop of atoms in the x-y plane around a central atom may be different from that in the x-z plane; the central atom may be bound tightly in the x-y plane, but loosely in the x-z plane. This gives rise to a local shear stress, τ_i.[9] Similarly, local elastic moduli, B_i the local bulk modulus and G_i the local shear modulus, can be defined.[10]

It was found that in the high-temperature liquid state the fluctuations in local pressure are related to temperature in a very simple manner

$$\frac{V\langle p^2\rangle}{2B} = \frac{kT}{4}, \qquad (3)$$

where $\langle\cdots\rangle$ is a thermal and temporal or ensemble average, $V=\langle V\rangle$, $B=\langle B\rangle$ and k is the Boltzmann constant.[11] This means that the total potential energy of the system, $3NkT/2$, where N is the number of atoms, is well described as the sum of the local elastic energy due to the atomic level stresses,[10] and it is equally divided among the six stress components, pressure and five shear stresses, that represent local topological fluctuations. However, Eq. (3) extrapolates to zero at $T=0$, which means that all the atomic bond lengths have to be equal to the ideal length at $T=0$, whereas it is impossible to achieve such a state in real metallic glasses because of topological frustration.[10,17] This means that the system will not be able to achieve thermal equilibrium at low temperatures and becomes nonergodic, in other words kinetically freezes into a glassy structure, below a certain temperature which defines the glass transition. Thus in our earlier paper[13] we used Eq. (3) to define the glass transition temperature, T_g, by

$$\frac{kT_g}{4} = \frac{V\langle p_{\mathrm{crit}}^2\rangle}{2B} = \frac{BV}{2}\langle\varepsilon_{\mathrm{crit}}^2\rangle. \qquad (4)$$

The basis of Eq. (3) is that the atomic level stresses are totally localized, and the stresses at neighboring sites are uncorrelated. However, when the system is frozen this assumption is no longer valid, and the local stress produces a

TABLE I. The Poisson's ratio, ν, atomic volume, V, values of T_g and B for various metallic glasses. The values of ν and B at T_g were evaluated by the procedure described in the Appendix. The data for compositions without a reference are unpublished results.

Metallic glasses	T_g (K)	$V=M/\rho$ cm^3/mol	$\nu(T_g)$	$B(T_g)V$ (eV/atom)	$\nu(RT)$	$B(RT)V$ (eV/atom)
$Fe_{64}Cr_4Mo_5W_2Zr_8Y_2B_{15}$	898	7.3	0.291	10.13	0.27	10.74
$Fe_{55}Mn_{10}Mo_{12}Er_2C_{15}B_6$ (Ref. 30)	813	6.77	0.295	9.67	0.28	10.17
$Ca_{55}Mg_{18}Zn_{11}Cu_{16}$	392	18.24	0.310	4.90	0.305	5.08
$Ca_{65}Mg_{15}Zn_{20}$	375	20.96	0.310	4.84	0.310	5.06
$Nd_{60}Al_{10}Fe_{20}Co_{10}$ (Ref. 31)	485	15.2	0.313	7.14	0.310	7.32
$Ce_{70}Al_{10}Ni_{10}Cu_{10}$ (Ref. 32)	359	16.9	0.316	4.68	0.310	4.73
$Ca_{50}Mg_{20}Zn_{30}$	400	17.19	0.317	5.06	0.311	5.20
$Fe_{48}Cr_{15}Mo_{14}Er_2C_{15}B_6$ (Ref. 30)	843	6.72	0.325	12.58	0.310	13.23
$Y_{36}Sc_{20}Al_{24}Ni_{10}Co_{10}$	650	13.7	0.338	9.17	0.326	9.58
$Mg_{60}Cu_{30}Y_{10}$	423	12.6	0.339	6.67	0.33	6.81
$Mg_{70}Ca_5Zn_{25}$ (Ref. 33)	393	13.28	0.341	6.48	0.34	6.63
$Ti_{40}Zr_{25}Cu_{12}Ni_3Be_{20}$ (Ref. 34)	604	9.84	0.352	10.27	0.345	10.60
$Zr_{46.75}Ti_{8.25}Cu_{7.5}Ni_{10}Be_{27.5}$ (Ref.35)	622	9.93	0.358	11.14	0.35	11.52
$Zr_{41.2}Ti_{13.8}Cu_{12.5}Ni_{10}Be_{22.5}$ (Ref.36)	625	10	0.358	10.51	0.35	10.88
$Zr_{41}Ti_{14}Cu_{12.5}Ni_{10}Be_{22.5}$ (Ref. 37)	620	10	0.360	11.43	0.35	11.82
$Zr_{48}Nb_8Cu_{12}Fe_8Be_{24}$ (Ref. 37)	658	10.2	0.367	11.57	0.36	11.99
$Pr_{60}Cu_{20}Ni_{10}Al_{10}$ (Ref. 38)	409	9.93	0.367	7.04	0.36	7.16
$Zr_{50}Cu_{37}Al_{10}Pd_3$	706	11.09	0.376	12.44	0.364	12.85
$Zr_{50}Cu_{40}Al_{10}$	706	10.87	0.378	12.60	0.369	13.21
$Cu_{60}Zr_{20}Hf_{10}Ti_{10}$ (Ref. 37)	754	9.51	0.379	11.95	0.369	12.61
$Zr_{50}Cu_{30}Ni_{10}Al_{10}$	710	10.66	0.380	12.67	0.370	13.23
$Zr_{52.5}Cu_{17.9}Ni_{14.6}Al_{10}Ti_5$	686	11.00	0.382	12.77	0.373	13.28
$Pd_{40}Cu_{30}Ni_{10}P_{20}$ (Ref. 39)	561	8.01	0.400	11.61	0.393	12.06
$(Pd_{0.2}Ni_{0.8})_{80}P_{20}$ (Ref. 40)	602	6.95	0.403	11.73	0.396	12.23
$Pd_{39}Cu_{30}Ni_{10}P_{21}$ (Ref. 41)	586	7.97	0.404	12.58	0.40	13.13
$(Pd_{0.4}Ni_{0.6})_{80}P_{20}$ (Ref. 40)	588	7.45	0.406	12.88	0.40	13.39
$(Pd_{0.7}Fe_{0.3})_{80}P_{20}$ (Ref. 40)	612	8.0	0.407	12.83	0.401	13.36
$(Pd_{0.6}Ni_{0.4})_{80}P_{20}$ (Ref. 40)	585	7.74	0.410	13.64	0.403	14.17
$(Pd_{0.75}Fe_{0.25})_{80}P_{20}$ (Ref. 40)	617	8.14	0.410	13.31	0.404	13.87
$(Pd_{0.8}Fe_{0.2})_{80}P_{20}$ (Ref. 40)	630	8.32	0.410	13.36	0.404	13.96
$(Pd_{0.85}Fe_{0.15})_{80}P_{20}$ (Ref. 40)	643	8.44	0.413	13.22	0.407	13.82
$(Pd_{0.8}Ni_{0.2})_{80}P_{20}$ (Ref. 40)	590	8.28	0.415	14.20	0.41	14.75
$Pd_{77.5}Cu_6Si_{16.5}$ (Ref. 40)	636	8.74	0.416	15.24	0.411	15.81
$(Pt_{0.8}Ni_{0.2})_{75}P_{25}$ (Ref. 40)	485	8.51	0.423	17.40	0.42	17.81
$Pt_{57.5}Ni_{5.3}Cu_{14.7}P_{22.5}$ (Ref. 41)	508	8.77	0.424	17.58	0.42	18.05

long-range stress field to contain it.[10,11] This long-range stress field can be calculated in the continuum approximation using Eshelby theory.[18] For the local pressure the total elastic energy is given by

$$E_v = \frac{V\langle p^2\rangle}{2B}K_\alpha = \frac{BV}{2K_\alpha}\langle(\varepsilon_v^T)^2\rangle, \tag{5}$$

$$K_\alpha = \frac{3(1-\nu)}{2(1-2\nu)}, \tag{6}$$

where ε_v^T is the volume strain before the environment relaxes (transformation strain).[10] The energy to create such local density or pressure fluctuation, E_v, must be related to the glass transition temperature. By combining Eqs. (4) and (5) we may express T_g by

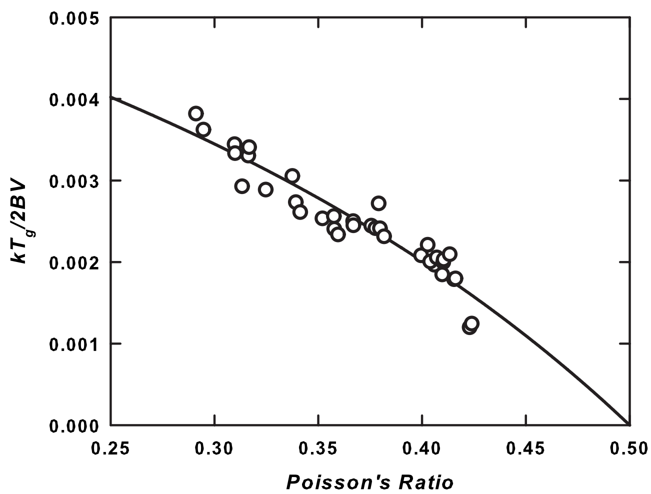

FIG. 1. Glass transition temperature, T_g, multiplied by $k/(2BV)$, as Eq. (1), plotted as a function of the Poisson's ratio for various metallic glasses listed in Table I. The values of ν and B used here are evaluated at T_g, corrected by the procedure described in the Appendix. The solid line indicates $(\varepsilon_v^T)^2/K_\alpha$, as in Eq. (7), with ε_v^T=0.095.

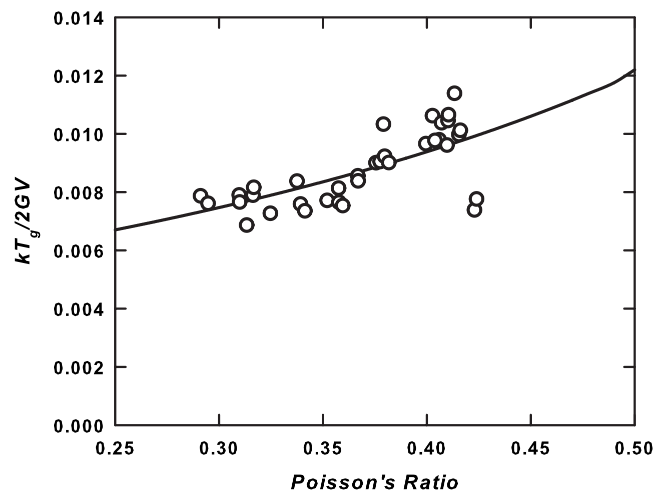

FIG. 2. The same data as Fig. 1, but expressed as $kT_g/2GV$. The values of ν and G used here are at T_g, corrected by the procedure described in the Appendix. The solid line indicates Eq. (7), with ε_v^T=0.095.

$$\frac{kT_g}{4} = E_v^{\rm crit} = \frac{BV}{2K_\alpha}(\varepsilon_v^{T,\rm crit})^2, \quad \frac{kT_g}{2BV} = \frac{(\varepsilon_v^{T,\rm crit})^2}{K_\alpha}. \tag{7}$$

On the other hand it has been suggested that the glass transition temperature is proportional to the shear modulus G (Ref. 19) and the Young's modulus E.[20] Below these ideas are compared to the recent experimental values of the glass transition temperature and elastic moduli, and we show that Eq. (7) best describes the glass transition temperature.

III. COMPARISON WITH EXPERIMENTAL DATA

For a long time metallic glasses available were thin ribbons produced by rapid quenching, and thus reliable values of elastic moduli to test these theories were not attainable. But recently the development of bulk metallic glasses and the resonant ultrasound spectroscopy (RUS) technique[21] made it possible to determine B and G separately with high accuracy. Using recent data on metallic glasses, supplementing them with our own unpublished data obtained with the RUS measurements as tabulated in Table I we examined the relationship between the glass transition temperature and the elastic moduli. We plot the results as a function of Poisson's ratio, ν, stimulated by the suggestion by Novikov and Sokolov[22] that the fragility coefficient[23] is related to ν. Usually the RUS measurements are made at room temperature, while the elastic moduli that relate to the glass transition have to be evaluated at T_g by extrapolating the data below T_g. This effect is small, amounting only to a few percent. But for the sake of completeness we have estimated the values of elastic moduli at T_g as described in the Appendix.

First to examine the validity of Eq. (4) we plot the ratio $kT_g/2BV$ against ν in Fig. 1. If Eq. (4) is correct the value of $kT_g/2BV$ should be independent of ν. Instead, Fig. 1 shows a strong correlation between $kT_g/2BV$ and ν, suggesting that T_g depends not only on B but on both B and G. The plot of $kT_g/2GV$ against ν is shown in Fig. 2. This plot shows a weaker dependence on ν, but $kT_g/2GV$ is not constant. A similar plot for $kT_g/2E$ is shown in Fig. 3 (above). However, for a dimensional reason kT_g should be related, if any, to EV rather than to E. Indeed the plot of $kT_g/2EV$ in Fig. 3 (be-

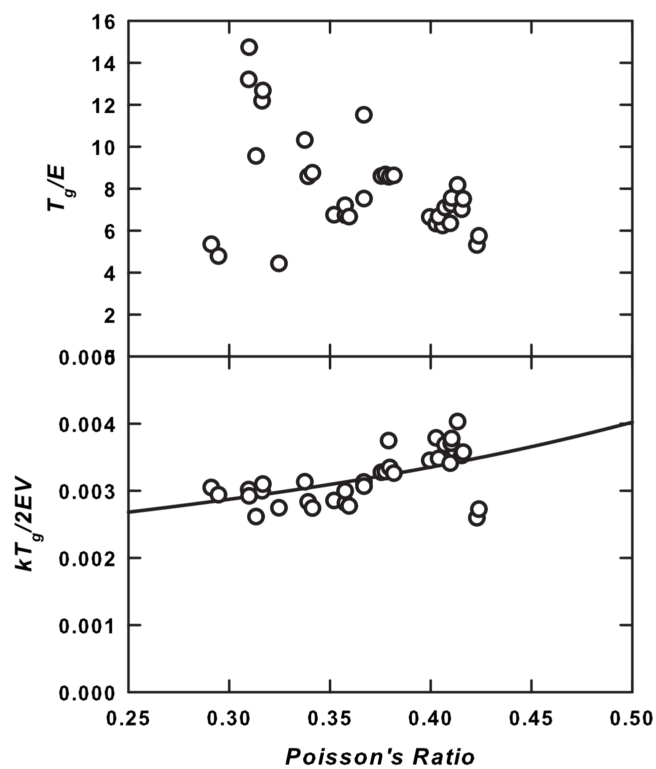

FIG. 3. The same data as Fig. 1, but expressed as T_g/E (above, in the units of K/GPa) and $kT_g/2EV$ (below). The values of ν and E used here are at T_g, corrected by the procedure described in the Appendix. The solid line in the lower figure indicates Eq. (7), with ε_v^T=0.095.

low) shows a much better correlation. Among these plots in Figs. 1–3 EV shows the strongest correlation with kT_g. However, Young's modulus describes a response of a free object to uniaxial stress, which is not consistent with the fluctuations of a continuous network. Moreover, these plots suggest that kT_g is not a function of a single parameter, such as BV, GV, or EV, but depends on both BV and GV, or equivalently on BV and ν. Figs. 1–3 show also Eq. (7) as solid curves. It is evident that Eq. (7) describes the experimental data excellently, with the value of $\varepsilon_v^{T,\mathrm{crit}}$ equal to 0.095 ± 0.004. As far as we know this is the first time that the glass transition temperature, quantitatively expressed in terms of measurable variables, was shown to agree with a wide range of experimental data.

IV. CRITICAL STRAIN

Equation (7) which explains the data so well has a single parameter ε_v^{Tg}, in addition to the measurable parameters, B, V, and ν. To explain the physical meaning of ε_v^{Tg} and to deduce its value let us go back to Eq. (1). As we discussed earlier in DRP glasses for an atom to fit into the site with a certain value of N_C it has to be elastically strained by $\varepsilon_v^T = 3\Delta x = 3(x_{N_c} - 1)$, which is the transformation strain in the Eshelby theory.[18] By expanding Eq. (1) with Δx around $x = 1$, it is given by

$$\varepsilon_v^T = 3\Delta x = 3\Delta N_C \Bigg/ \left. \frac{\partial N_C(x)}{\partial x} \right|_{x=1} = \frac{3\Delta N_C}{2\pi}(2\sqrt{3} - 3), \tag{8}$$

where $\Delta N_C = N_C(x) - N_C(1)$. The critical increment of N_C for the topological instability, $\Delta N_C = 0.5$, gives the local critical volume strain, $\varepsilon_v^{T,\mathrm{crit}} = 0.11$. This means that if the local transformation volume strain is larger than 11% or smaller than −11% the site is topologically unstable, and the local coordination number may change. For this reason these sites are *liquidlike*, whereas the sites with the volume strain less than 11% in magnitude are *solidlike*. Since the atomic level volume strain ε_v has a Gaussian distribution,[24] the fraction of the liquidlike atomic sites, $p(liq)$, is given by the complementary error function, $CE(y_c)$, where $y_c = \varepsilon_v^{T,\mathrm{crit}} / \sqrt{2}\langle(\varepsilon_v^T)^2\rangle^{1/2}$. For the standard deviation of the Gaussian distribution $\langle(\varepsilon_v^T)^2\rangle^{1/2}$ equal to $\varepsilon_v^{Tg} = 0.095$ as in Figs. 1–3, $y_c = 0.825$. This means that the total fraction of the *liquidlike* sites is given by $p(liq) = CE(y_c) = 0.243$. This value is in the range of the percolation limit for the DRP structure, which is estimated to be $p_c = 0.198$ for $N_C = 12.18$ and $p_c = 0.246$ for $N_C = 8.73$.[25] This result implies that the glass transition occurs through the percolation transition of the liquidlike states, as predicted by Cohen and Grest.[26] The value of $p(liq)$ is slightly higher than the estimate for $N_C = 12$, but it probably originates from the kinetic nature of the glass transition that it slightly depends upon the cooling rate. The exact percolation concentration may predict the ideal glass transition temperature (Kauzmann temperature) rather than the real glass transition temperature.

Based upon these results, we suggest that Eq. (7), deduced by the topological fluctuation theory, predicts the glass transition temperature without a sample dependent adjustable parameter. Currently the most successful theory to describe the behavior of liquids is the mode-coupling theory (e.g., Ref. 4). However, the mode-coupling theory requires input from the experimental data for each composition. In comparison the current theory needs only the knowledge of the elastic moduli and atomic volume which can be determined from the interatomic potentials or directly from the first principles,[27] thus bringing about the predictive capability. As we demonstrate here this relatively simple model is capable of quantitatively expressing the glass transition temperature with high accuracy.

V. CONCLUSIONS

Understanding the mechanism of the glass transition at an atomistic level is challenging because it is difficult enough to describe the atomistic dynamics of liquid. We found earlier that the atomic level stresses provide a good description of the local structural fluctuations in liquids through their local elastic energy. This description, however, fails below a certain temperature because of the topological frustration of the local structure, and we propose that this deviation from the equilibrium defines the glass transition. Through this logic we derived an expression of the glass transition temperature, and found that it agrees excellently with the wide range of experimental data without an adjustable parameter. The success reported here suggests that this approach may be extended to more complex glasses, and could form the basis for a long-sought general microscopic theory of liquids and glasses.

ACKNOWLEDGMENTS

The authors gratefully acknowledge useful and insightful discussions with J. C. Phillips, V. N. Novikov, W. L. Johnson, C. A. Angell, L. Battezzati, A. L. Greer, S. J. L. Billinge, R. Hermann, C. T. Liu, and J. R. Morris. This work at the University of Tennessee and Oak Ridge National Laboratory was supported by the U.S. Department of Energy under Contract No. DE-AC05-00OR-22725, and by the National Science Foundation, DMR-0506292. The work at the University of Virginia was supported by the DARPA under ONR Grant No. N00014-01-1-0961.

APPENDIX

Elastic moduli of a solid depend on temperature because of the anharmonicity of interatomic interaction. For crystalline solids this dependence is well described by a phenomenological expression by Varshni[28]

$$C(T) = C_0 - \frac{s}{e^{\theta_D/T} - 1}, \tag{A1}$$

where $C(T)$ is an elastic modulus at temperature T, θ_D is the Debye temperature, and the value of s is chosen so that $C(T_m) = 0.55\ C(0)$, with T_m being the melting temperature. We found[29] that Eq. (A1) works for metallic glasses as well, provided that we assume $B(T_m)=0.78\ B(0)$ for bulk modulus and $G(T_m)=0.55\ G(0)$ for shear modulus. T_m was evaluated as a compositional average of the melting temperature of the components, rather than the actual melting temperature of the crystalline compound. The actual melting temperature depends on the delicate balance in the free energy between the solid and liquid, and is lowered by frustration near the eutectic composition. Elastic moduli, however, do not exhibit strong composition dependence, and follow more closely the composition dependence of the Debye temperature. Thus the compositional average of the melting temperature of the constituent elements provides a better energy scale for the elastic moduli. As shown in Table I the effect of this correction is small. If the elastic moduli measured at room temperature were used in evaluating Eq. (7), we obtain $\varepsilon_v^{T,\mathrm{crit}}=0.092\pm0.003$ rather than 0.095 ± 0.004, and $p(liq)=0.227$ rather than 0.243. Thus this effect is within the margin of error. Volume expansion between room temperature and T_g is even smaller, of the order of 0.1%, and was not considered in this work.

[1] P. W. Anderson, Science **267**, 1615 (1995).
[2] P. G. Debenedetti and F. H. Stillinger, Nature (London) **410**, 259 (2001).
[3] W. Götze and L. Sjögren, Rep. Prog. Phys. **55**, 241 (1992).
[4] S. P. Das, Rev. Mod. Phys. **76**, 785 (2004).
[5] E. B. Warren, *X-Ray Diffraction* (Addison-Wesley, Reading, 1969; Dover, New York, 1990).
[6] J. L. Finney, Proc. R. Soc. London **319**, 479 (1970).
[7] J. D. Honeycutt and H. C. Andersen, J. Phys. Chem. **91**, 4950 (1987).
[8] D. Turnbull and M. H. Cohen, J. Phys. Chem. **34**, 120 (1960).
[9] T. Egami, K. Maeda, and V. Vitek, Philos. Mag. A **41**, 883 (1980).
[10] T. Egami and D. Srolovitz, J. Phys. F: Met. Phys. **12**, 2141 (1982).
[11] S.-P. Chen, T. Egami, and V. Vitek, Phys. Rev. B **37**, 2440 (1988).
[12] T. Egami and Y. Waseda, J. Non-Cryst. Solids **64**, 113 (1984).
[13] T. Egami, Mater. Sci. Eng., A **226**, 261 (1997).
[14] J. D. Bernal, Nature (London) **188**, 910 (1960); G. D. Scott, *ibid.* **188**, 908 (1960).
[15] T. Egami and S. Aur, J. Non-Cryst. Solids **89**, 60 (1987).
[16] The ideal radius of the sphere to fit an icosahedron made of 12 spheres of radius unity is 0.91. However, since the space cannot be filled with icosahedra alone, when an icosahedron is embedded in the DRP structure it becomes distorted. Thus the ideal atomic size for $N_C=12$ is more correctly given by Eq. (1), than the size of a sphere that fits a perfect icosahedron.
[17] D. R. Nelson, Phys. Rev. B **28**, 5515 (1983).
[18] J. D. Eshelby, Proc. R. Soc. London **241**, 376 (1957).
[19] J. C. Dyre, N. B. Olsen, and T. Christensen, Phys. Rev. B **53**, 2171 (1996).
[20] A. Inoue and A. Takeuchi, Mater. Trans. **43**, 1892 (2002).
[21] A. Migliori, J. L. Sarrao, W. M. Visscher, T. M. Bell, M. Lei, Z. Fisk, and R. G. Leisure, Physica B **183**, 1 (1993).
[22] V. N. Novikov and A. P. Sokolov, Nature (London) **431**, 961 (2004).
[23] C. A. Angell, Science **267**, 1924 (1995).
[24] D. Srolovitz, K. Maeda, V. Vitek, and T. Egami, Philos. Mag. A **44**, 847 (1981).
[25] M. J. Powell, Phys. Rev. B **21**, 3725 (1980).
[26] M. H. Cohen and G. S. Grest, Phys. Rev. B **20**, 1077 (1979).
[27] O. H. Nielsen and R. M. Martin, Phys. Rev. B **32**, 3780 (1985).
[28] Y. P. Varshni, Phys. Rev. B **2**, 3952 (1970).
[29] Z. Zhang, V. Keppens, and T. Egami (unpublished).
[30] V. Ponnambalam, S. J. Poon, and G. J. Shiflet, J. Mater. Res. **19**, 3046 (2004).
[31] Z. Zhang, R. J. Wang, L. Xia, B. C. Wei, D. Q. Zhao, M. X. Pan, and W. H. Wang, J. Phys.: Condens. Matter **15**, 4503 (2003).
[32] B. Zhang, M. X. Pan, D. Q. Zhao, and W. H. Wang, Appl. Phys. Lett. **85**, 61 (2004).
[33] X. Gu, G. J. Shiflet, and S. J. Poon, J. Mater. Res. **20**, 1935 (2005).
[34] F. Q. Guo, S. J. Poon, and G. J. Shiflet, Appl. Phys. Lett. **86**, 091907 (2005).
[35] W. H. Wang, C. Dong, and C. H. Shek, Mater. Sci. Eng., R. **44**, 45 (2004).
[36] C. J. Gilbert, V. Schroeder, and R. O. Ritchie, Mat. Res. Soc. Symp. Proc. Vol. 554 (Mater. Res. Soc., Warrendale, PA, 1999), p. 343.
[37] Y. Zhang, Y. F. Ji, D. Q. Zhao, Y. X. Zhuang, R. J. Wang, M. X. Pan, Y. D. Dong, and W. H. Wang, Scr. Mater. **44**, 1107 (2001).
[38] Z. F. Zhao, Z. Zhang, P. Wen, M. X. Pan, D. Q. Zhao, W. H. Wang, and W. L. Wang, Appl. Phys. Lett. **82**, 4699 (2003).
[39] N. Nishiyama, A. Inoue, and J. Z. Jiang, Appl. Phys. Lett. **78**, 1985 (2001).
[40] H. S. Chen, J. Non-Cryst. Solids **18**, 157 (1975).
[41] L. M. Wang, Z. J. Zhan, D. Y. Dai, L. L. Sun, and W. K. Wang, Appl. Phys. Lett. **77**, 1147 (2000).